J|A|C|S
ARTICLES
Published on Web 11/05/2002

Probing Transport and Microheterogeneous Solvent Structure in Acetonitrile−Water Mixtures and Reversed-Phase Chromatographic Media by NMR Quadrupole Relaxation

Erica D. Dawson and Scott L. Wallen*

Contribution from the Kenan and Venable Laboratories, Department of Chemistry, CB#3290, The University of North Carolina, Chapel Hill, North Carolina 27599-3290

Received June 7, 2002

Abstract: Mixtures of CH_3CN and H_2O are the predominant solvent systems used in reversed-phase liquid chromatographic (RPLC) separations, as well as in a multitude of other applications. In addition, acetonitrile is the simplest model for an amphiphilic molecule possessing both organic and polar functional groups. Although many studies have focused on this solvent system, the general nature of the intermolecular interactions are not fully understood, and a microscopic description of the proposed microheterogeneity that exists is still not clearly established. In the present study, we measure the spin−lattice relaxation times (T_1) of ^{14}N to determine reorientational correlation times (τ_c) of CH_3CN-H_2O solvent mixtures over the entire binary composition range and at temperatures ranging from 25.0 to 80.0 °C. At all compositions, the microscopic observable, τ_c, is found to be directly proportional to the macroscopic solution viscosity when scaled for temperature (η/T). This indicates that for a constant composition, this system's dynamics are well described by hydrodynamic theory on a microscopic level. These results suggest that under appropriate conditions, the measurement of changes in quadrupolar relaxation times is a reliable means of determining changes in solution viscosity. We stress the importance of this approach in systems not amenable to traditional viscosity measurements, such as those having species in interfacial regions. This approach is used to examine the changes in the interfacial solution viscosity of CH_3CN-H_2O mixtures in contact with a commercially available C_{18}-bonded stationary phase. The measurements indicate that CH_3CN is motionally hindered at the stationary phase surface. The surface affected CH_3CN has a larger dependence of τ_c on temperature than the bulk CH_3CN, indicating greater changes in the interfacial viscosity as a function of temperature. Additionally, the bulk relaxation data show direct correlations to existing models of proposed regions of structure for CH_3CN-H_2O mixtures. Using a microscopic hydrodynamic approach, we show that, quite unexpectedly, each of the experimentally determined parameters in the viscosity correlation plots change simultaneously, and we propose that these are indicative of changes in the distribution of species for this microheterogeneous liquid system. Although distinct regions for the onset of microheterogeneity have previously been proposed, within the framework of a microscopic hydrodynamic model and the recently proposed model of Reimers and Hall,[1] the present data support the existence of a microheterogeneous solvent structure that varies continuously over the full range of temperatures and compositions examined.

Introduction

Mixtures of CH_3CN and H_2O constitute a widely used aqueous-organic system for applications ranging from electrochemistry to synthesis. Additionally, CH_3CN-H_2O mixtures in contact with alkyl-bonded stationary phases are the most commonly employed and useful chromatographic systems and are indispensable with respect to the reversed-phase liquid chromatographic (RPLC) separation of many polar molecules including most biomolecules. Understanding mobile phase speciation, the nature of solvation in the bulk and in contact with the stationary phase, and mobile phase/stationary phase interactions are important for establishing a unified mechanistic retention model. Though it is known that the alkyl stationary phase plays an important role in the retention of solutes and that it is insufficient to explain a separation in terms of the differing solubility of solutes in the mobile phase alone, the mechanisms of retention are still not fully understood. Most theoretical separation models include both partition and adsorption components, and although the subject of RPLC retention mechanisms will not be discussed in depth here, the reader is directed to literature reviews on the subject.[2−7]

* To whom correspondence should be addressed. E-mail: wallen@email.unc.edu.

(1) Reimers, J. R.; Hall, L. E. *J. Am. Chem. Soc.* **1999**, *121*, 3730−3744.
(2) Gilpin, R. K. *Anal. Chem.* **1985**, *57*, 1465A−1474A.
(3) Dorsey, J. G.; Dill, K. A. *Chem. Rev.* **1989**, *89*, 331−346.
(4) Jaroniec, M. *J. Chromatogr.* **1993**, *656*, 37−50.
(5) Lochmueller, C. H.; Reese, C.; Aschman, A. J.; Breiner, S. J. *J. Chromatogr.* **1993**, *656*, 3−18.
(6) Dorsey, J. G.; Cooper, W. T. *Anal. Chem.* **1994**, *66*, 857A−867A.
(7) Vailaya, A.; Horvath, C. *J. Chromatogr. A* **1998**, *829*, 1−27.

10.1021/ja027226h CCC: $22.00

Researchers have employed numerous methods to probe the interactions important in understanding the separation process. Studies examining the properties of the mobile phase in the presence of numerous stationary phases have been conducted, and others have concentrated on investigating properties of the stationary phase under a wide array of thermodynamic conditions. Various spectroscopic methods including fluorescence,[8−23] Raman,[24−29] IR,[30] UV−vis,[15] small angle neutron scattering,[31] sum frequency generation,[32,33] and NMR[34−49] have been used to probe the mobile and stationary phases, as well as the composition, structure, and dynamics of the chromatographic interface. An underlying theme in a number of these works is the apparent reduction in the rate of molecular transport of the mobile phase system near the chromatographic interface.[13,17−19,21−23,37,45−49] The development of thermally stable stationary phases and high temperature RPLC techniques has made investigations of chromatographic interfaces at elevated temperatures increasingly important,[50−55] and yet to date, the effects of temperature on the transport properties of the surface-affected mobile phase have not been elucidated.

As mentioned above, NMR spectroscopy has been used to study the structure and dynamics of bulk solvent mixtures as well as the interfacial region in RPLC systems. One experiment commonly employed is the measurement of the longitudinal or spin−lattice (T_1) relaxation times of quadrupolar nuclei. Quadrupolar nuclei have an advantage with respect to exploring dynamics in that their relaxation is dominated by interaction of the quadrupole moment (Q) of the nucleus of interest with the local electric field gradient (q). As a result, measured T_1 values for nuclei such as ^{2}H (deuterium) and ^{14}N can provide a direct measure of molecular reorientation relative to a particular bond axis. In the motionally narrowed regime ($\omega\tau_c \ll 1$), the measured T_1 can be related to the reorientational correlation time (τ_c) according to[56]

$$\frac{1}{T_1} = \frac{3\pi^2}{10}\frac{2I+3}{I^2(2I-1)}\left(1+\frac{\eta_q^2}{3}\right)\left(\frac{eQq}{h}\right)\tau_c(\theta) = \frac{3\pi^2}{2}\chi^2\tau_c(\theta) \quad (1)$$

where θ is the angle between the vector containing the pertinent relaxation interaction (along the bond axis of the quadrupolar nucleus in the present case) and the symmetry axis of the molecule. The nuclear spin quantum number (I) = 1, the asymmetry parameter (η_q) = 1 for the ^{14}N nucleus in CH_3CN, e is the fundamental unit of electrical charge, Q is the quadrupole moment, and h is Planck's constant. By consolidating the terms related to the quadrupole interaction into the quadrupolar coupling constant, $\chi = eQq/h$, τ_c is directly proportional to the inverse of the spin−lattice relaxation time as shown on the right-hand side of eq 1. This equation is an important starting point for examining solution dynamics, but it is important to understand that changes in τ_c with varying solution thermodynamics (e.g., composition, temperature, and pressure) can affect molecular interactions that ultimately control transport, partitioning, and separation.

Traditional Stokes−Einstein hydrodynamic theory can be useful in describing the solution dynamics of a relatively large spherical solute in a small, continuous solvent according to

$$\tau_c = \frac{V_h\eta}{kT} \quad (2)$$

where V_h is the hydrodynamic volume, η is viscosity, k is Boltzmann's constant, and T is absolute temperature. This familiar relationship does not necessarily apply to molecular systems in which the solute size approaches that of the surrounding solvent. The strict "stick" boundary condition inherent in this theory in which the solute's rotation does not impose any frictional force on the surrounding solvent molecules breaks down on a molecular scale. Solute−solvent interactions, structural, and dynamic features of the solvent can cause this "stick" boundary condition to become more "slip"-like in that the rotation of the solute molecule does in fact bring about movement of the surrounding solvent molecules. Many researchers have been successful in modifying this traditional

(8) Lochmuller, C. H.; Marshall, D. B.; Wilder, D. R. *Anal. Chim. Acta* **1981**, *130*, 31−43.
(9) Lochmueller, C. H.; Marshall, D. B.; Harris, J. M. *Anal. Chim. Acta* **1981**, *131*, 263−269.
(10) Hunnicutt, M. L.; Harris, J. M.; Lochmueller, C. H. *J. Phys. Chem.* **1985**, *89*, 5246−5250.
(11) Carr, J. W.; Harris, J. M. *J. Chromatogr.* **1989**, *481*, 135−146.
(12) Men, Y. D.; Marshall, D. B. *Anal. Chem.* **1990**, *62*, 2606−2612.
(13) Wirth, M. J.; Burbage, J. D. *Anal. Chem.* **1991**, *63*, 1311−1317.
(14) Montgomery, M. E., Jr.; Green, M. A.; Wirth, M. J. *Anal. Chem.* **1992**, *64*, 1170−1175.
(15) Rutan, S. C.; Harris, J. M. *J. Chromatogr.* **1993**, *656*, 197−215.
(16) Waite, S. W.; Marshall, D. B.; Harris, J. M. *Anal. Chem.* **1994**, *66*, 2052−2061.
(17) Zulli, S. L.; Kovaleski, J. M.; Zhu, X. R.; Harris, J. M.; Wirth, M. J. *Anal. Chem.* **1994**, *66*, 1708−1712.
(18) Hansen, R. L.; Harris, J. M. *Anal. Chem.* **1995**, *67*, 492−498.
(19) Hansen, R. L.; Harris, J. M. *Anal. Chem.* **1996**, *68*, 2879−2884.
(20) Burns, J. W.; Bialkowski, S. E.; Marshall, D. B. *Anal. Chem.* **1997**, *69*, 3861−3870.
(21) Wirth, M. J.; Swinton, D. J. *Anal. Chem.* **1998**, *70*, 5264−5271.
(22) Swinton, D. J.; Wirth, M. J. *Anal. Chem.* **2000**, *72*, 3725−3730.
(23) Ludes, M. D.; Wirth, M. J. *Anal. Chem.* **2002**, *74*, 386-393.
(24) Thompson, W. R.; Pemberton, J. E. *Anal. Chem.* **1994**, *66*, 3362−3370.
(25) Doyle, C. A.; Vickers, T. J.; Mann, C. K.; Dorsey, J. G. *J. Chromatogr., A* **1997**, *779*, 91−112.
(26) Ho, M.; Cai, M.; Pemberton, J. E. *Anal. Chem.* **1997**, *69*, 2613−2616.
(27) Ho, M.; Pemberton, J. E. *Anal. Chem.* **1998**, *70*, 4915−4920.
(28) Doyle, C. A.; Vickers, T. J.; Mann, C. K.; Dorsey, J. G. *J. Chromatogr. A* **2000**, *877*, 25−39.
(29) Doyle, C. A.; Vickers, T. J.; Mann, C. K.; Dorsey, J. G. *J. Chromatogr. A* **2000**, *877*, 41−59.
(30) Sander, L. C.; Callis, J. B.; Field, L. R. *Anal. Chem.* **1983**, *55*, 1068−1075.
(31) Sander, L. C.; Glinka, C. J.; Wise, S. A. *Anal. Chem.* **1990**, *62*, 1099−1101.
(32) Wolf, L. K.; Yang, Y. J.; Pizzolatto, R. L.; Messmer, M. C. *ACS Symposium Series* **2001**, *781*, 293−305.
(33) Pizzolatto, R. L.; Yang, Y. J.; Wolf, L. K.; Messmer, M. C. *Anal. Chim. Acta* **1999**, *397*, 81−92.
(34) Gangoda, M. E.; Gilpin, R. K. *J. Magn. Reson.* **1983**, *53*, 140−143.
(35) Gilpin, R. K.; Gangoda, M. E. *J. Chromatogr. Sci.* **1983**, *21*, 352−361.
(36) Gilpin, R. K.; Gangoda, M. E. *Anal. Chem.* **1984**, *56*, 1470−1473.
(37) Marshall, D. B.; McKenna, W. P. *Anal. Chem.* **1984**, *56*, 2090−2093.
(38) Gilpin, R. K.; Gangoda, M. E. *J. Magn. Reson.* **1985**, *64*, 408−413.
(39) Miller, M. L.; Linton, R. W.; Maciel, G. E.; Hawkins, B. L. *J. Chromatogr.* **1985**, *319*, 9−21.
(40) Gangoda, M.; Gilpin, R. K.; Fung, B. M. *J. Magn. Reson.* **1987**, *74*, 134−138.
(41) Gangoda, M.; Gilpin, R. K.; Figueirinhas, J. *J. Phys. Chem.* **1989**, *93*, 4815−4818.
(42) Gangoda, M. E.; Gilpin, R. K. *Langmuir* **1990**, *6*, 941−944.
(43) Zeigler, R. C.; Maciel, G. E. *J. Phys. Chem.* **1991**, *95*, 7345−7353.
(44) Zeigler, R. C.; Maciel, G. E. *J. Am. Chem. Soc.* **1991**, *113*, 6349−6358.
(45) Ellison, E. H.; Marshall, D. B. *J. Phys. Chem.* **1991**, *95*, 808−813.
(46) Bliesner, D. M.; Sentell, K. B. *Anal. Chem.* **1993**, *65*, 1819−1826.
(47) Bliesner, D. M.; Sentell, K. B. *J. Chromatogr.* **1993**, *631*, 23−35.
(48) Sentell, K. B. *J. Chromatogr.* **1993**, *656*, 231−263.
(49) Wysocki, J. L.; Sentell, K. B. *Anal. Chem.* **1998**, *70*, 602−607.
(50) Carr, P. W.; Doherty, R. M.; Kamlet, M. J.; Taft, R. W.; Melander, W.; Horvath, C. *Anal. Chem.* **1986**, *58*, 2674−2680.
(51) Li, J.; Carr, P. W. *Anal. Chem.* **1996**, *68*, 2857−2868.
(52) Li, J.; Carr, P. W. *Anal. Chem.* **1997**, *69*, 837−843.
(53) Li, J.; Hu, Y.; Carr, P. W. *Anal. Chem.* **1997**, *69*, 3884−3888.
(54) Yan, B.; Zhao, J.; Brown, J. S.; Blackwell, J.; Carr; Peter, W. *Anal. Chem.* **2000**, *72*, 1253−1262.
(55) Thompson, J. D.; Carr, P. W. *Anal. Chem.* **2002**, *74*, 1017−1023.
(56) Abragam, A. *Principles of Nuclear Magnetism*; Oxford University Press: New York, 1961.

theory to include a continuum of boundary conditions and for solutes of varying shape and size in order to better explain experimental data from a number of techniques.[57−59] Kivelson points out that one can postulate a microscopic hydrodynamic model that is not derived from first principles but is useful in describing a system's dynamics in terms of temperature and its relation to the solution viscosity

$$\tau_c = \frac{V_h \kappa}{k}\left(\frac{\eta}{T}\right) + \tau_0 \qquad (3)$$

where V_h is the hydrodynamic volume, κ is the McClung−Kivelson constant and represents the ratio of anisotropic, intermolecular interactions to the overall intermolecular interactions and is related to the degree of coupling between rotational and translational motion, k is Planck's constant, η is viscosity, T is absolute temperature, and τ_0 is the zero viscosity intercept.[60−62] The appearance of the finite, zero-viscosity intercept has been attributed to an inertial contribution to τ_c, as τ_0 has been related to the correlation time of a classical free rotor $(2\pi/9)(\sqrt{I/kT})$ where I is the moment of inertia.[63−66] From a purely hydrodynamic point of view, there is not a justification for the inclusion of τ_0, however, this form of the Kivelson equation has proven useful to describe liquid molecular dynamics. An alternate approach has been the idea that deviations from traditional hydrodynamic theory are due to changes in the volume of the reorienting species. This can be introduced by modifying V_h in eq 2 as $V_h = V_m f C$,[67] where V_m is the molecular volume, f is a calculable friction coefficient that depends on the shape of the solute, and C is a coefficient which is dependent on the boundary conditions of the system.[57,58]

Interpretations of molecular reorientation have been successful using a framework resting on the traditional hydrodynamic approach, however, the large majority of cases have been in systems that involve no specific interactions (such as hydrogen bonding) between the reorientational probe molecule and the solvent system, or in which the solute probe is much larger than the surrounding solvent molecules.[59,67,68] Within the class of strongly interacting systems there are far fewer examples in which a traditional hydrodynamic approach offers a reasonable description of the solution transport properties. It is from this microscopic hydrodynamic point of view that we hypothesize that measurements of reorientational correlation time (τ_c) can provide a reliable measure of changes in viscosity as a function of thermodynamic state for a given composition, and this hypothesis is tested in the present work.

Measurements of T_1 by NMR will provide an average τ_c that is weighted according to the distribution of spins in different environments present in the system. One can envision the mobile phase components in a RPLC system present in two distinct environments: a bulk solvent environment, and one in which the mobile phase components are interacting with the alkyl-bonded stationary phase near the surface. If there is rapid exchange on the NMR time scale, it should be possible to extract information specifically about the mobile phase species interacting with the surface according to[70]

$$\tau_{obs} = \tau_{bulk} + \frac{2d}{R}(\tau_{surface} - \tau_{bulk}) \qquad (4)$$

where τ_{obs} is the observed reorientational correlation time for the sample, τ_{bulk} is the measured reorientational correlation time for the bulk solvent environment, $\tau_{surface}$ is the average reorientational correlation time for those mobile phase species interacting with the stationary phase, d is the thickness of the surface-associated layer, and R is the pore radius. Such two-state models have been used successfully by Jonas and co-workers[71−75] in NMR and optical studies and by Fourkas and co-workers[76−78] in optical Kerr effect (OKE) spectroscopy studies to examine the dynamics of liquids confined within the pores of silica sol−gel xerogels. Within a hydrodynamic framework, the relation given in eq 3 should allow one to relate changes in the microscopically determined bulk and surface τ_c values to the respective changes in the bulk and surface-affected viscosities. This approach allows us to make comparisons of the temperature dependence of the changes in viscosity of bulk and surface associated species.

A variety of investigations of the CH_3CN-H_2O binary mixture in the absence of a chromatographic stationary phase have also been conducted in an attempt to develop a concise picture of the solvation structure and dynamics that exist as a function of composition. A number of approaches including thermodynamic studies,[79−88] NMR,[89−94] UV−vis,[95,96] fluorescence,[97] IR,[98,99]

(57) Hu, C.-M.; Zwanzig, R. *J. Chem. Phys.* **1974**, *60*, 4354−4357.
(58) Dote, J. L.; Kivelson, D.; Schwartz, R. N. *J. Phys. Chem.* **1981**, *85*, 2169−2180.
(59) Ben-Amotz, D.; Drake, J. M. *J. Chem. Phys.* **1988**, *89*, 1019−1029.
(60) McClung, R. E. D.; Kivelson, D. *J. Chem. Phys.* **1968**, *49*, 3380−3391.
(61) Fury, M.; Jonas, J. *J. Chem. Phys.* **1976**, *65*, 2206−2210.
(62) Kivelson, D. *Faraday Symp. Chem. Soc.* **1977**, *11*, 7−25.
(63) Alms, G. R.; Bauer, D. R.; Brauman, J. I.; Pecora, R. *J. Chem. Phys.* **1973**, *59*, 5310−5320.
(64) Alms, G. R.; Bauer, D. R.; Brauman, J. I.; Pecora, R. *J. Chem. Phys.* **1973**, *58*, 5570−5578.
(65) Bauer, D. R.; Alms, G. R.; Brauman, J. I.; Pecora, R. *J. Chem. Phys.* **1974**, *61*, 2255−2261.
(66) Bauer, D. R.; Brauman, J. I.; Pecora, R. *J. Am. Chem. Soc.* **1974**, *96*, 6840−6843.
(67) Morresi, A.; Sassi, P.; Ombelli, M.; Paliani, G.; Cataliotti, R. S. *Phys. Chem. Chem. Phys.* **2000**, *2*, 2857−2861.
(68) Whittenburg, S. L.; Wang, C. H. *J. Chem. Phys.* **1977**, *66*, 4255−4262.
(69) Bopp, T. T. *J. Chem. Phys.* **1967**, *47*, 3621−3626.
(70) Brownstein, K. R.; Tarr, C. E. *J. Magn. Reson.* **1977**, *26*, 17−24.
(71) Liu, G.; Li, Y.; Jonas, J. *J. Chem. Phys.* **1989**, *90*, 5881−5882.
(72) Liu, G.; Mackowiak, M.; Li, Y.; Jonas, J. *Chem. Phys.* **1990**, *149*, 165−171.
(73) Liu, G.; Li, Y.; Jonas, J. *J. Chem. Phys.* **1991**, *95*, 6892−6901.
(74) Zhang, J.; Jonas, J. *J. Phys. Chem.* **1993**, *97*, 8812−8815.
(75) Wallen, S. L.; Nikiel, L.; Yi, J.; Jonas, J. *J. Phys. Chem.* **1995**, *99*, 15421−15427.
(76) Loughnane, B. J.; Farrer, R. A.; Fourkas, J. T. *J. Phys. Chem. B* **1998**, *102*, 5409−5412.
(77) Loughnane, B. J.; Scodinu, A.; Farrer, R. A.; Fourkas, J. T.; Mohanty, U. *J. Chem. Phys.* **1999**, *111*, 2686−2694.
(78) Loughnane, B. J.; Farrer, R. A.; Scodinu, A.; Reilly, T.; Fourkas, J. T. *J. Phys. Chem. B* **2000**, *104*, 5421−5429.
(79) Moreau, C.; Douheret, G. *Thermochim. Acta* **1975**, *13*, 385−392.
(80) Moreau, C.; Douheret, G. *J. Chem. Thermodyn.* **1976**, *8*, 403−410.
(81) De Visser, C.; Heuvelsland, W. J. M.; Dunn, L. A.; Somsen, G. *J. Chem. Soc., Faraday Trans. 1* **1978**, *74*, 1159−1169.
(82) Easteal, A. J. *Aust. J. Chem.* **1980**, *33*, 1667−1675.
(83) Easteal, A. J.; Woolf, L. A. *J. Chem. Thermodyn.* **1982**, *14*, 755−762.
(84) Davis, M. I. *Thermochim. Acta* **1983**, *63*, 67−82.
(85) Davis, M. I.; Douheret, G. *Thermochim. Acta* **1986**, *104*, 203−222.
(86) Davis, M. I.; Douheret, G. *Thermochim. Acta* **1987**, *116*, 183−194.
(87) Easteal, A. J.; Woolf, L. A. *J. Chem. Thermodyn.* **1988**, *20*, 693−699.
(88) Easteal, A. J.; Woolf, L. A. *J. Chem. Thermodyn.* **1988**, *20*, 701−706.
(89) Hertz, H. G.; Zeidler, M. D. *Ber. Bunsen-Ges. Physik. Chem.* **1964**, *68*, 821−837.
(90) Von Goldammer, E.; Hertz, H. G. *J. Phys. Chem.* **1970**, *74*, 3734−3755.
(91) Easteal, A. J. *Aust. J. Chem.* **1979**, *32*, 1379−1384.
(92) Leiter, H.; Patil, K. J.; Hertz, H. G. *J. Solution Chem.* **1983**, *12*, 503−517.
(93) Leiter, H.; Albayrak, C.; Hertz, H. G. *J. Mol. Liq.* **1984**, *27*, 211−225.
(94) Hardy, E. H.; Zygar, A.; Zeidler, M. D. *Z. Phys. Chem.* **2000**, *214*, 1633−1657.
(95) Balakrishnan, S.; Easteal, A. J. *Aust. J. Chem.* **1981**, *34*, 943−947.
(96) Nigam, S.; De Juan, A.; Stubbs, R. J.; Rutan, S. C. *Anal. Chem.* **2000**, *72*, 1956−1963.
(97) Easteal, A. J. *Aust. J. Chem.* **1979**, *32*, 271−275.

Raman,[100] sum frequency generation (SFG),[101] molecular dynamics simulations,[102,103] and ab initio calculations[1] have been utilized to investigate this important solvent system. Although controversial spectroscopic assignments, differing interpretations of similar spectroscopic data, and the lack of full characterization as a function of temperature and pressure have hindered a thorough description of the solvent mixture, these studies do provide a wealth of data from techniques covering different experimental time scales and regions of the electromagnetic spectrum that must be reconciled within a single framework.

A large number of these studies invoke a model of CH_3CN-H_2O mixtures initially put forth by Moreau and Douhéret[79] which hypothesizes microheterogeneous solvent structure and the existence of three distinct structural regions: a H_2O-rich region from $0 < \chi_{CH_3CN} < 0.15-0.2$ (χ_{CH_3CN} = mole fraction of CH_3CN) where CH_3CN molecules occupy small voids in the water structure, an intermediate region of "microheterogeneity" from 0.15 to 0.2 $< \chi_{CH_3CN} <$ 0.75−0.8 where small separate clusters of the two substances are proposed to exist, and an CH_3CN-rich region from 0.75 to 0.8 $< \chi_{CH_3CN} < 1$ where water molecules occupy cavities between CH_3CN molecules. More recently, a comprehensive study of CH_3CN dissolved in many different solvents using Raman spectroscopy and ab initio calculations was performed by Reimers and Hall under ambient conditions.[1] In a large section of their paper devoted to CH_3CN-H_2O interactions and solvent structure, Reimers and Hall propose that the microheterogeneity is not switched on and off at discrete concentrations due to drastic changes in the structure. Instead their data indicate that the system experiences a continuous microheterogeneity over the entire solvent composition with the changes simply being that each component has solvent clusters that grow or shrink with respect to each other depending on the solution composition.

Remembering that T_1 measurements from NMR will result in a τ_c weighted by the number of spins existing in different environments, a two-state model similar to that mentioned for a chromatographic system can be applied to bulk CH_3CN-H_2O mixtures. We assume that CH_3CN exists in a "free" state where it is not hydrogen bonded to H_2O, and in a "bound" state where it is hydrogen bonded to H_2O. This leads to an equation of the form

$$\tau_{obs} = f\,\tau_{free} + (1 - f)\tau_{bound} \qquad (5)$$

where τ_{free} and τ_{bound} represent the reorientational correlation times of the free and bound CH_3CN, with mole fractions f and $1 - f$, respectively. This approach is similar to the interpretation of Raman data for the ν_2 stretching mode of CH_3CN in mixtures with H_2O by Reimers and Hall.[1] It is important to point out that the designation of *free* CH_3CN does not indicate that it is completely *unbound* in solution, but that it is *not* hydrogen bonded to H_2O. We use this relation to deconvolute the observed NMR relaxation data and determine the relative populations of these two species. A comparison of the populations derived from the NMR data in the present study to the room-temperature Raman data of Reimers and Hall is made.

In light of its widespread use in RPLC, it is of interest to examine the liquid dynamics and transport properties of both bulk CH_3CN-H_2O solvent and the CH_3CN-H_2O-alkyl stationary phase system as a function of composition at elevated temperatures using NMR quadrupolar relaxation measurements. The present study investigates the dynamics of CH_3CN-H_2O mixtures in the bulk solvent mixture over the full range of mobile phase compositions and at temperatures ranging from 25.0 to 80.0 °C through the use of ^{14}N T_1 measurements of CH_3CN. These results will be discussed in light of previous studies on the structure and dynamics of this solvent mixture. Experimental evidence shows a direct correlation between the microscopic relaxation data and the solution viscosity within a hydrodynamic framework (eq 3) over the entire binary composition range. Most previous NMR studies have concentrated on ^2H T_1 relaxation as an indicator of changes in viscosity. Comparison of the present results with previous work gives an indication of the inaccuracy of the ^2H relaxation measurements without special precautions and we have discussed these issues in a recent paper.[104] We definitively establish the use of ^{14}N relaxation measurements as a means of accurately detecting viscosity changes in such systems. We have also examined the ^{14}N T_1 times of the CH_3CN-H_2O-alkyl stationary phase system as a function of temperature. Equation 4 is used to separate the relaxation of species in the bulk from those associated with the stationary phase. A comparison is made between the changes in viscosity that occur in the bulk and surface species as a function of increasing temperature. The reliability of using this method to follow changes in viscosity of a liquid (i.e., mobile phase system) at an interface (i.e., the stationary phase) will also be discussed with respect to the uncertainties in the thickness of the surface associated CH_3CN layer.

Materials and Methods

Chemicals. H_2O (Fisher, HPLC Grade) was used as received. CH_3CN (Aldrich, 99.93%, HPLC Grade) was dried with molecular sieve (Fisher, type 4 Å) and otherwise used as received. The C_{18}-bonded silica stationary phase (Vydac, type 218TPB2030) is a polymeric, nonendcapped stationary phase with an average particle size of 20−30 μm, 300 Å average pore diameter, specific surface area of 100−125 m^2/g (from the manufacturer), and a bonding density of 4.12 μmol/m^2 (as determined by %C analysis).

NMR Measurements. Measurements were made on both Bruker Avance 400 and 500 MHz spectrometers operating at 28.50 and 35.67 MHz, respectively, for the ^{14}N nucleus. A Bruker 5 mm broadband probe was used on the 400 MHz spectrometer, and a Nalorac 5 mm broadband probe was used on the 500 MHz instrument. The preacquisition delay ($d1$) was in excess of $5T_1$ for all experiments. Spectra were acquired without a deuterium lock, as there is not an appreciable drift in the magnetic field over the time required for a typical experiment. Sample temperature was calibrated using a type J−K−T thermocouple (Omega Engineering, model HH21) and controlled to within ±0.1 °C using the Eurotherm BVT3000 temperature controller supplied with the spectrometer. Temperature was allowed to equilibrate between experiments.

The normal inversion recovery sequence (180°−τ−90°-acquire) was employed using 16 delay times, and T_1 was calculated by fitting the peak intensity as a function of delay time to a 3 parameter single exponential within the Bruker Avance software. As a precaution, T_1

(98) Eaton, G.; Pena-Nunez, A. S.; Symons, M. C. R. *J. Chem. Soc., Faraday Trans. 1* **1988**, *84*, 2181−2193.
(99) Takamuku, T.; Tabata, M.; Yamaguchi, A.; Nishimoto, J.; Kumamoto, M.; Wakita, H.; Yamaguchi, T. *J. Phys. Chem. B* **1998**, *102*, 8880−8888.
(100) Rowlen, K. L.; Harris, J. M. *Anal. Chem.* **1991**, *63*, 964−969.
(101) Zhang, D.; Gutow, J. H.; Eisenthal, K. B.; Heinz, T. F. *J. Chem. Phys.* **1993**, *98*, 5099−5101.
(102) Kovacs, H.; Laaksonen, A. *J. Am. Chem. Soc.* **1991**, *113*, 5596−5605.
(103) Mountain, R. D. *J. Phys. Chem. A* **1999**, *103*, 10 744−10 748.
(104) Dawson, E. D.; Wallen, S. L. *Anal. Chem.* **2002**, *74*, 5333−5336.

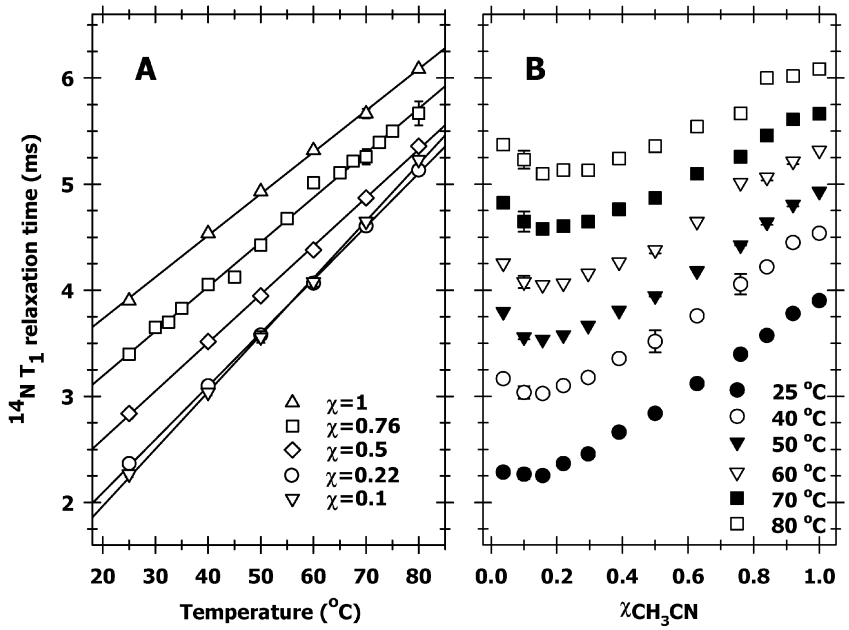

Figure 1. (A)^{14}N T_1 relaxation times versus temperature for selected CH_3CN-H_2O compositions, χ = mole fraction CH_3CN. (B)^{14}N T_1 relaxation times versus composition at all temperatures investigated.

was also obtained using an alternate manual procedure to ensure accuracy of this method, and was found to be within 5% of the value calculated using the Bruker software.

Sample Preparation. For bulk solvent samples, not in contact with stationary phase, CH_3CN and H_2O mixtures were volumetrically prepared at various compositions of the two solvents with a calibrated pipet in small sample vials and mixed well before transferring to clean, dry 5 mm outer diameter (o.d.) NMR tubes (Wilmad). The ^{14}N T_1 relaxation times for samples in which the solvents were used as received were compared to samples that had been degassed with four freeze−pump−thaw cycles and subsequently sealed to investigate the effects of dissolved O_2 on the measured relaxation times. Differences in relaxation times for the two types of samples were well below the root-mean-square deviation (RSD) associated with the T_1 measurement and differences were not statistically significant. As a result, no degassing step was employed in further sample preparations.

In the experiments involving stationary phase, solvent mixtures as prepared above were added to a nominal amount of stationary phase in each case. Experiments were performed at $\chi_{CH_3CN} \geq 0.5$ as the mobile phase is unable to wet the stationary phase at ambient conditions below this composition. Slurries of the mobile phase solvent and the stationary phase were mixed well using a vortex mixer and sonication. The slurry was then pipetted into a 3 mm o.d. insert, and the 3 mm insert was placed inside a centrifuge tube and spun in a swinging bucket centrifuge (IEC Centra CL2) at 2500 rpm until the height of the packed bed of stationary phase was constant. The height of the packed stationary phase was well above the coil region, and the solvent layer was kept well above the packed bed. The 3 mm tube was then covered with Parafilm and inserted into a 5 mm NMR tube and tightly capped.

Results and Discussion

1. Dynamics and Transport Properties. Figure 1A shows the ^{14}N T_1 relaxation times as a function of temperature for five different CH_3CN-H_2O compositions of the twelve investigated. Error bars represent ±1 standard deviation of triplicate measurements, and are smaller than the symbol width used in some cases. A comprehensive table containing T_1, τ_c, $D_\perp$, and η at all compositions and temperatures investigated is available as Supporting Information. A constant value for the quadrupolar coupling parameter (χ) of 3.74 MHz was used[105] for all conditions investigated to calculate τ_c from eq 1. One should note that recent reports by Farrar et al.[106−116] indicate that χ can vary with temperature and solvent composition and that an accurate determination of the changes can be obtained through a combination of ab initio calculations and modeling of NMR data. In light of the present results, we did not focus on this approach in this work, although its relevance is discussed in a later section with respect to the validity of eq 3.

The linear increase in ^{14}N T_1 corresponds to a decrease in τ_c according to Equation 1, and indicates both increased reorientational motion of CH_3CN and an expected decrease in the number of intermolecular interactions as kT increases. ^{14}N T_1 relaxation times for pure CH_3CN as a function of temperature were measured in early studies on the dynamics and anisotropic rotation of CH_3CN.[69,117−119] These previous studies show linear increases in T_1 with temperature, and where comparisons are possible with the present results, differences are less than ±10%. It is noted that although T_1 linearly increases as a function of temperature over the entire composition range, the isocompo-

(105) Bull, T. E.; Jonas, J. *J. Chem. Phys.* **1970**, *53*, 3315−3317.
(106) Ludwig, R.; Weinhold, F.; Farrar, T. C. *J. Chem. Phys.* **1995**, *103*, 6941−6950.
(107) Ludwig, R.; Weinhold, F.; Farrar, T. C. *J. Chem. Phys.* **1995**, *103*, 3636−3642.
(108) King, B. F.; Farrar, T. C.; Weinhold, F. *J. Chem. Phys.* **1995**, *103*, 348−352.
(109) Stringfellow, T. C.; Farrar, T. C. *J. Chem. Phys.* **1995**, *102*, 9465−9473.
(110) Ludwig, R.; Bohmann, J.; Farrar, T. C. *J. Phys. Chem.* **1995**, *99*, 9681−9686.
(111) Ludwig, R.; Weinhold, F.; Farrar, T. C. *J. Phys. Chem. A* **1997**, *101*, 8861−8870.
(112) Wendt, M. A.; Farrar, T. C. *Molecular Physics* **1998**, *95*, 1077−1081.
(113) Wendt, M. A.; Zeidler, M. D.; Farrar, T. C. *Mol. Phys.* **1999**, *97*, 753−756.
(114) Ferris, T. D.; Zeidler, M. D.; Farrar, T. C. *Mol. Phys.* **2000**, *98*, 737−744.
(115) Hansen, M. J.; Wendt, M. A.; Farrar, T. C. *J. Phys. Chem. A* **2000**, *104*, 5328−5334.
(116) Ferris, T. D.; Farrar, T. C. *Molecular Physics* **2002**, *100*, 303−309.
(117) Moniz, W. B.; Gutowsky, H. S. *J. Chem. Phys.* **1963**, *38*, 1155−1162.
(118) Woessner, D. E.; Snowden, J., B. S.; Strom, E. T. *Mol. Phys.* **1968**, *14*, 265−273.
(119) Bull, T. E. *J. Chem. Phys.* **1975**, *62*, 222−226.

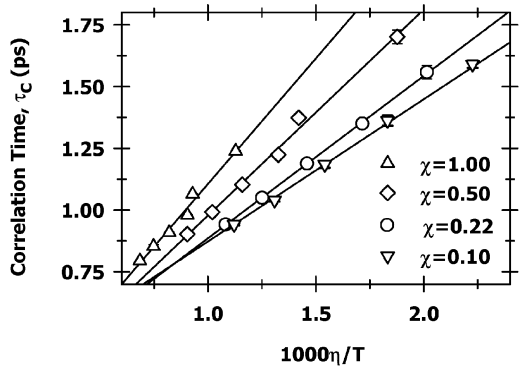

Figure 2. Reorientational correlation time, τ_c, versus $1000\eta/T$ showing the correlation between the microscopic observable and the macroscopic viscosity for various solution compositions.

sition lines in Figure 1A overlap as the mole fraction of CH_3CN in the system is decreased (compare $\chi_{CH_3CN} = 0.22$ and $\chi_{CH_3CN} = 0.10$). This overlap is indicative of a "turnover" if the various isotherms are plotted as a function of χ_{CH_3CN} as in Figure 1B. A minimum in T_1 can be seen at $0.1 < \chi_{CH_3CN} < 0.2$ for each isotherm examined, and increased temperatures show a more dramatic turnover than the data recorded at 25.0 °C. Previously, ^{14}N T_1 relaxation times were measured over the entire CH_3CN-H_2O binary composition range at 25 °C by von Goldammer and Hertz.[90] These values agree with the present data to within 10% and show similar T_1 behavior as a function of composition. In a recent study focusing on the investigation of isotope effects on reorientation and the factors that influence anisotropic reorientation in CH_3CN-H_2O at the critical concentration, Hardy et al.[94] investigated the relaxation of ^1H, ^2H, ^{13}C, and ^{14}N in this mixture. Their ^{14}N measurements were limited to one composition ($\chi_{CH_3CN} = 0.36$) as a function of temperature, and showed a linear increase in the relaxation time for temperatures ranging from 7 to 25 °C.

As one of our goals is to examine the compositions over which a linear dependence of τ_c on η/T exists (eq 3) and to investigate the validity of a hydrodynamic approach for the determination of viscosity changes using NMR, we plot the τ_c determined from ^{14}N T_1 values versus $1000\eta/T$ for several isocomposition lines in Figure 2.

Viscosities of CH_3CN-H_2O mixtures at 25.0 and 40.0 °C were linearly interpolated from previously published results.[120] Viscosities at 50.0, 60.0, 70.0, and 80.0 °C were calculated from the relation developed by Chen and Horváth[121] relating the viscosities of CH_3CN-H_2O mixtures to the composition and temperature in the range from 30.0 to 120.0 °C. Figure 2 clearly shows a linear correlation with the bulk viscosity when scaled for temperature. Although 12 compositions were investigated and this linear trend exists for all 12, only four mole fractions over the entire binary composition range are shown for clarity. The experimental parameters determined from the linear regressions for all compositions are discussed later. The linear correlation between τ_c and η/T is predicted from the microscopic hydrodynamic model given in eq 3, but in systems in which strong interactions such as hydrogen bonding are present, this approach does not often accurately describe the solution transport properties under varying temperature conditions. The ^{14}N data presented, however, provides strong evidence that the CH_3CN-H_2O system is well-represented by this microscopic hydrodynamic model. One should note that this equation is valid only under isocomposition conditions for this system, and that a full description within this context is not currently possible as observed from the differing slopes of the isocomposition lines. One possible cause of this is the fact that χ may be dependent on the composition of the binary mixture. Because our goal was to show that changes in the τ_c value could be correlated with η/T under isocomposition conditions, we have not made an effort to quantify these differences, however, they will be discussed in the section focused on the solution species' composition. The data above, however, support the hypothesis that changes in the microscopic τ_c obtained from NMR measurements can be used to accurately determine changes in viscosity of this mixture as a function of changing thermodynamic conditions at constant solution composition. In contrast to the results from a previous ^2H investigation,[47] the current ^{14}N data clearly show that the CH_3CN does not experience a homogeneous solution environment over the entire binary composition range but that it changes continuously from dilute CH_3CN to neat CH_3CN.

In addition to studies of the bulk CH_3CN-H_2O solvent mixture, there has been interest in the examination of the viscosity of different fluids in regions affected by interfacial forces. The first study employing NMR quadrupolar T_1 relaxation times as a probe of the interactions at a chromatographic interface, performed by Marshall and McKenna,[37] reported the ^2H T_1 relaxation times of H_2O in CH_3CN-H_2O mixtures as a function of composition from 0 to 50% H_2O in both the neat mobile phase and in mobile phase-stationary phase slurries. The authors correlate their results of a decrease in the T_1 relaxation times of H_2O to the reduction in motional freedom of the H_2O under different conditions. Ellison and Marshall[45] later attempted to make a more quantitative analysis of the "fluidity" at the interface of this system by measuring the ^2H and ^{14}N T_1 relaxation times of CH_3CN in contact with a commercially available C_{18} stationary phase and a bare silica surface under ambient conditions. In this study, a two-state fast exchange model was used to obtain surface relaxation times of the CH_3CN from the measured T_1 values, and by applying hydrodynamic theory, this relaxation was related to an apparent increase in the viscosity of the CH_3CN at the surface of the stationary phase. Studies under changing solution conditions or at elevated temperatures, however, were not examined.

Expanding upon this work, Sentell and co-workers[46,47,49] have also examined mobile phase-stationary phase interactions using NMR T_1 relaxation measurements in a number of different mobile phase mixtures. They focused on room-temperature measurements of the ^2H T_1 relaxation times of CH_3CN and H_2O over the entire binary composition range both in the bulk and in contact with two C_{18} stationary phases having very different bonding densities at room temperature in order to qualitatively gauge the degree of association of the CH_3CN with the different stationary phases. They report an "essentially constant" T_1 for CH_3CN in the bulk mixture over the entire binary composition range, and put forth the hypothesis that their results indicate that CH_3CN is in a relatively homogeneous solution environment in mixtures with H_2O over the entire binary composition range. Their ^2H T_1 data does not scale with the viscosity of the bulk

(120) Wode, H.; Seidel, W. *Ber. Bunsen-Ges. Phys. Chem.* **1994**, *98*, 927−934.
(121) Chen, H.; Horvath, C. *Anal. Methods Instrum.* **1994**, *1*, 213−222.

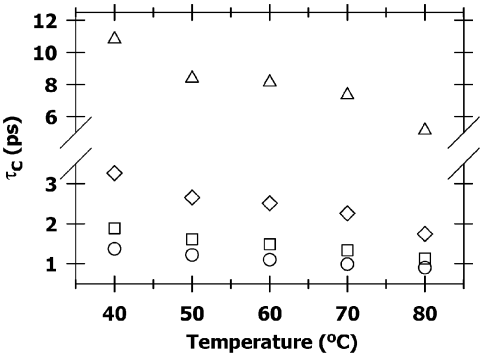

Figure 3. CH_3CN reorientational correlation times, τ_c, of $\chi_{CH_3CN} = 0.5$ in bulk solvent mixtures (τ_{bulk}, ○), in contact with stationary phase, (τ_{obs}, □), and $\tau_{surface}$ values calculated using a two-state fast exchange model for CH_3CN-H_2O mixtures in contact with stationary phase, assuming a surface affected layer thickness, d, of 4.09 Å (△) and 20.45 Å (◇).

liquid mobile phase, and this raises issues of the validity of the technique in providing information on the viscosity of either the bulk fluid mixture or of the system in contact with the stationary phase. Figure 1B, however, shows a continuous change in the ^{14}N T_1 of CH_3CN in this mixture as a function of composition at all temperatures examined.

We have previously made measurements of ^2H T_1 relaxation times of these same CH_3CN-H_2O mixtures and observed nonmonotonic changes as a function of temperature.[104] We have found that convective motion at elevated temperatures had a tremendous effect on the measured T_1 due to the long ^2H T_1 values (~s). This difficulty in measuring accurate ^2H T_1 times motivated the present ^{14}N T_1 measurements, which we have found to be reproducible as indicated by the error bars in Figure 1. In fact, the largest %RSD for triplicate samples is less than 1.8%. The high precision in the measured T_1 indicates the reliability in using changes in T_1 of the ^{14}N nucleus to examine solvent transport and structural properties.

In addition to the bulk measurements, we have also measured the ^{14}N T_1 relaxation times of CH_3CN in CH_3CN-H_2O mixtures in contact with an alkyl C_{18}-bonded stationary phase. In Figure 3, we present a comparison of the reorientational correlation times determined in the bulk solvent mixture (τ_{bulk}) and the observed reorientational correlation time (τ_{obs}) for $\chi_{CH_3CN} = 0.5$ as a function of temperature. There is an average %RSD in the ^{14}N T_1 values for the solvent-stationary phase samples (used to calculate τ_{obs}) of approximately 6.2%. This increase compared to the bulk solvent measurements is attributed to the heterogeneous nature of the sample and the fact that the ^{14}N resonances are significantly broadened due to the solid stationary phase in the coil region. We have utilized the two-state fast exchange model in eq 4 to determine the reorientational correlation time of CH_3CN in the surface-affected layer ($\tau_{surface}$), and these results are also shown in Figure 3.

Examination of eq 4 indicates that measurements of both τ_{bulk} and τ_{obs} as well as values for R, the pore radius, and d, the "thickness" of the surface-associated layer, are needed to calculate $\tau_{surface}$. Both τ_{bulk} and τ_{obs} are determined directly from the measured ^{14}N T_1 relaxation times of the bulk solvent mixture (Figure 1A) and of the solvent mixture in contact with the stationary phase, respectively. As previously stated, many studies have focused on understanding the exact structure and nature of the stationary phase with respect to thermodynamic conditions. These studies have in a general sense shown the stationary phase to be extremely dynamic, exhibiting structural and composition changes with varying experimental conditions, and that the overall response of the stationary phase to these changes is still largely unknown. It has been shown in CH_3CN-H_2O-alkyl stationary phase systems that the interfacial region at the stationary phase surface is enriched in the CH_3CN mobile phase component.[122−125] This does not imply the structure of the alkyl chains or that the interfacial region is made up of a simple distinct layer of CH_3CN, but shows that the stationary phase has an affinity for the organic mobile phase component. We hesitate to postulate a visual picture of this very complex region, but emphasize that there is a population of CH_3CN molecules whose dynamics will clearly be affected by interactions with the chromatographic surface. A direct measure of the thickness of this surface-associated layer of CH_3CN would be extremely useful for the present study and could be determined through techniques such as neutron reflectivity. This is beyond the scope of the present investigation, however, and we will therefore make an assumption concerning d. The $\tau_{surface}$ values have been calculated using two limiting values of $d = 4.09$ Å and 20.45 Å, corresponding to 1 and 5 times the hard sphere diameter of CH_3CN over the entire surface of the stationary phase. Although we have estimated the surface-affected layer, we stress that useful information regarding changes in τ_c and therefore viscosity when CH_3CN is in contact with a C_{18} stationary phase can be obtained. The $\tau_{surface}$ calculated using both limits are significantly longer than the bulk values, showing that the tumbling motion of CH_3CN is highly restricted when interacting with the stationary phase. Applying the microscopic hydrodynamic model presented in eq 3, this $\tau_{surface}$ can be related to the viscosity of CH_3CN in the surface affected layer that is 2−5 times greater than the bulk viscosity, depending on the chosen d value. At 25.0 °C, this result is qualitatively similar to that of Marshall and Ellison[45] who predicted a surface viscosity of CH_3CN of several times that found in the bulk. Figure 3 also shows the temperature dependence of the surface reorientational motion, and indicates that the viscosity of the surface-affected liquid undergoes larger changes as a function of temperature than does the bulk viscosity. Comparison of the slopes for the surface-associated data and the bulk solvent data reveals that the viscosity at the interface changes by 53% and 46% for $d = 4.09$ Å and $d = 20.45$ Å, respectively, compared to a change of 34% in the bulk solvent system. The application of the two-state fast-exchange model to relaxation measurements on different chromatographic systems and other analytically relevant systems, such as microemulsions, will be a focus of future studies. The present method of determining relative viscosity changes will allow the examination of the effects of partitioning and the resulting intermolecular interactions on transport and ultimately mechanisms of separation in these complex molecular systems.

2. Structural Aspects and Speciation in CH_3CN-H_2O Mixtures. The elucidation of the liquid structure and assignment of particular equilibrium species in CH_3CN-H_2O mixtures is important for the further development and validation of theories

(122) Scott, R. P. W.; Kucera, P. *J. Chromatogr.* **1977**, *142*, 213−232.
(123) Tilly-Melin, A.; Askemark, Y.; Wahlund, K. G.; Schill, G. *Anal. Chem.* **1979**, *51*, 976−983.
(124) McCormick, R. M.; Karger, B. L. *Anal. Chem.* **1980**, *52*, 2249−2257.
(125) Slaats, E. H.; Markovski, W.; Fekete, J.; Poppe, H. *J. Chromatogr.* **1981**, *207*, 299−323.

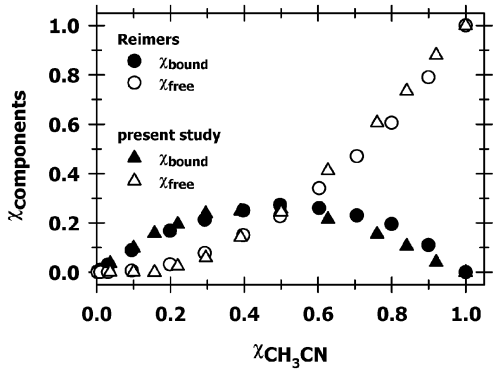

Figure 4. Free and bound mole fractions of CH_3CN calculated in bulk CH_3CN-H_2O mixtures assuming a two-state model for NMR data from the present study at 25.0 °C. Shown for comparison is data from Reimers and Hall[1] determined using Raman spectroscopy at 25.0 °C.

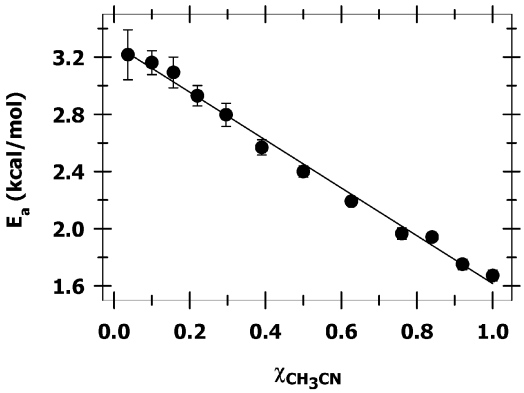

Figure 5. Activation energy (E_a) calculated from temperature-dependent behavior of reorientational correlation times (τ_c) as a function of mole fraction of CH_3CN in CH_3CN-H_2O mixtures.

regarding separation, provides experimental data for computational modeling, and allows one to consider the physical properties of the mixture from a microscopic point of view. With this in mind, we have applied the two-state population model in eq 5 to the present ^{14}N NMR relaxation data for the bulk solutions. This model fits the observed bulk reorientational correlation time into both "free" and "bound" CH_3CN, with each respective correlation time being weighted by the population of the species. This approach is analogous to that used by Reimers and Hall[1] to interpret Raman spectroscopic data at 25 °C as a function of composition in this mixture. Figure 4 shows the compositions of free and bound CH_3CN as a function of overall composition calculated from the present ^{14}N NMR data and from the Raman spectroscopic data of Reimers and Hall for the ν_2 vibrational band. Though the data presented are the result of two completely independent techniques that probe very different time scales, the observed populations of the free and bound species agree quite well over the entire binary composition range. A recent study using optical Kerr Effect Spectroscopy also revealed similar trends for CH_3CN in two environments as a function of composition.[126]

At low CH_3CN content, CH_3CN interactions with H_2O dominate as the amount of CH_3CN that is hydrogen bound to water increases steadily to intermediate compositions. It is evident from these data that until $\chi_{CH_3CN} \approx 0.2$ there are no detectable free CH_3CN molecules. Beyond this point, the concentration of CH_3CN increases, the CH_3CN-CH_3CN interactions become more abundant, and the fraction of free CH_3CN monotonically increases until at $\chi_{CH_3CN} = 0.5$ the free and bound components are equal. The monotonic increase in free CH_3CN above this composition continues as the CH_3CN-CH_3CN interactions become a much larger fraction of the overall interactions taking place. Due to the form of eq 5, this increase in the free CH_3CN component is obviously accompanied by a decrease in the fraction of bound CH_3CN.

The recent comprehensive study of CH_3CN in a variety of solvents by Reimers and Hall has provided new insight into the solution structure of this mixture. Their effort was focused on the development of an all-encompassing theory for the solution structure of CH_3CN by borrowing several robust features from existing analyses of experimental solvent shifts. They determined a set of possible structures from ab initio calculations, chose the most likely from energetic and experimental evidence, and compared the experimental solvent shifts to the structure's calculated solvent shift. In their section on CH_3CN-H_2O mixtures, they present Raman spectroscopic data of the ν_2 CN stretch as a function of composition at room temperature. One band appears at high CH_3CN concentration, and a blue-shifted band appears with decreasing concentration. The lower energy band is attributed to "free" CH_3CN, which they define as *not* being hydrogen bound to H_2O, and the higher energy band is attributed to "bound" CH_3CN which is hydrogen bonded to H_2O. They deconvolute the Raman spectra into two bands, and the corresponding "free" and "bound" populations as a function of χ_{CH_3CN} calculated from these Raman spectra are the data shown with the present NMR results in Figure 4. Reimers and Hall rationalize this observed behavior of the two CH_3CN species in terms of the forming and breaking of CH_3CN-H_2O interactions, writing simple equilibrium expressions for this model, and they obtain very close agreement between the populations calculated from the equilibrium model and observed Raman results. In contrast to earlier developed microheterogeneity models that propose sudden changes in structure occurring at specific compositions, their data support a microheterogeneity model in which no distinct onset of microheterogeneity exists as a function of composition. Rather, they propose that microheterogeneity is a continuous phenomenon that exists over the entire binary composition, with the structural changes occurring gradually as clusters of the two species shrink and grow with changing composition. Our NMR data also provides strong evidence for this view of the solution structure as discussed above with regard to Figure 4. Although Reimers and Hall present data at 25°C only, we have applied eq 5 to the temperature-dependent NMR data and present these results in the Supporting Information (Figure S1).

The Arrhenius activation energy (E_a) for the reorientation process at each composition can be determined from the slope of log T_1 versus inverse absolute temperature plots, and these E_a values for CH_3CN-H_2O as a function of composition are shown in Figure 5. Errors in E_a were determined through the usual propagation of errors, and the correlation coefficient (R^2) for Figure 5 is 0.993.

The experimentally determined E_a for pure CH_3CN of 1.67 kcal/mol sufficiently agrees with literature values for pure CH_3CN that range from 1.7 (±0.1) to 2.0 kcal/mol.[69,117,118] To

(126) Ernsting, N. P.; Photiadis, G. M.; Hennig, H.; Laurent, T. *J. Phys. Chem. A* **2002**, *106*, 9159−9173.

date, work by von Goldammer and Hertz[90] is the only report found that examines ^{14}N T_1 relaxation times for CH_3CN-H_2O mixtures over the entire binary composition range. This study, however, only examines the relaxation behavior from 5 to 35 °C. The present results are in good agreement with the activation energies calculated by von Goldammer and Hertz where comparisons are possible.

It is apparent from Figure 5 that the calculated E_a scales linearly as the amount of H_2O in the system is increased. In fact, the E_a for the reorientation of the CH_3CN increases by a factor of 2 in moving from pure CH_3CN to $\chi_{CH_3CN} = 0.0369$. This increase shows that CH_3CN is clearly more motionally hindered as the concentration of H_2O in the mixtures is increased. This is indicative of a steady increase in the number of CH_3CN-H_2O interactions present with decreasing CH_3CN content. Upon examination of eq S1 (see Supporting Information), τ_c is dependent on the angle (θ) the relaxation interaction of interest makes with the axis of symmetry for the molecule, and since $\theta = 0°$ for ^{14}N in CH_3CN, eq S1 reduces to eq S2. ^{14}N T_1 measurements of CH_3CN are therefore a probe of the perpendicular "tumbling" rotational diffusion coefficient, $D_\perp$, and likewise the E_a calculated from this reorientational process as a function of composition will be a probe of the activational barrier to this $D_\perp$ reorientation as the solution composition changes. Short-range CH_3CN-CH_3CN interactions are usually a result of CH_3CN molecules which are aligned antiparallel.[99] Dipolar alignment allows CH_3CN the ability to "tumble" relatively freely perpendicular to the molecule's axis of symmetry with minimal perturbation of the neighboring molecules. CH_3CN-H_2O interactions, however, typically involve hydrogen bonding with the nitrile group, an interaction that would greatly inhibit this $D_\perp$ motion due to the strong directionality of the interaction. The number of CH_3CN-H_2O interactions will increase as the composition of the mixture shifts toward predominantly H_2O, and there will be a corresponding decrease in the number of CH_3CN-CH_3CN interactions. We therefore see a steady increase in the E_a required for this $D_\perp$ reorientation as the concentration of CH_3CN decreases, with a limiting value of 3.22 ± 0.17 kcal/mol at the lowest χ_{CH_3CN}. This increase in the E_a as a function of increased H_2O concentration supports the data presented in Figure S1 that indicates increased temperatures perturb the population of CH_3CN-CH_3CN interactions more readily than CH_3CN-H_2O interactions. In fact, we see that the interaction can be assumed to be almost twice as large in the latter case based on the rotational barriers that are presented in Figure 5. Additionally, one can clearly see that there are no discrete changes in the values of E_a with the differing solution compositions. These results fully support the view that there is no distinct mole fraction that corresponds to the onset of microheterogeneity and provide strong evidence that the liquid structure continuously changes from infinitely dilute CH_3CN to neat CH_3CN.

Recall from Figure 2 that the ^{14}N T_1 relaxation times were linearly correlated with the bulk solution viscosity when scaled for temperature, and that this shows the applicability of the microscopic hydrodynamic model presented in eq 3 to CH_3CN-H_2O mixtures. Though the error in the measured T_1's are consistent at different compositions and temperatures, it was noted that the linearity of fit for the viscosity correlation was dependent on the solution composition and that the experimentally determined parameters from the linear fits in Figure 2 undergo consistent changes as a function of composition. We believe these changes could lend further support to the idea of structural microheterogeneity in CH_3CN-H_2O and explain these changes in the context of a microscopic hydrodynamic approach.

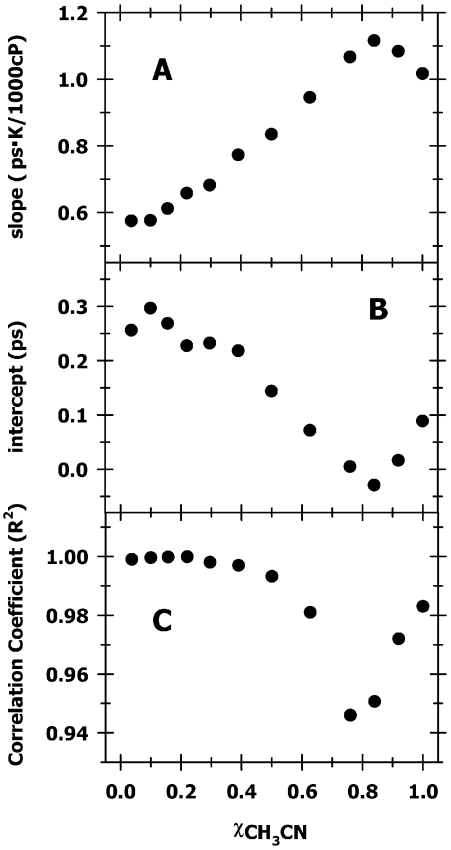

Figure 6. Plots of the experimental parameters of the least squares linear regression fits to viscosity plots (as in Figure 2) as a function of mole fraction of CH_3CN for all compositions investigated (A) slope, (B) y-intercept, and (C) correlation coefficient.

Figures 6A, B, and C show the slope, intercept and correlation coefficient (R^2) of the τ_c vs $1000\eta/T$ plots as a function of composition for each of the 12 compositions investigated. A distinct minimum or maximum occurs in all three figures at approximately $\chi_{CH_3CN} = 0.75-0.8$. Because the changes in these cannot be attributed to changes in the error of the measured T_1 times for these conditions, these changes must somehow reflect the average solution structure of the CH_3CN. Our hypothesis is that these changes are representative of the diversity of possible CH_3CN-H_2O structures in solution at these compositions. The different types of interactions possible in pure CH_3CN are limited to CH_3CN self-interactions. As the H_2O concentration increases, however, there is an increase in the number of ways that CH_3CN and H_2O can interact. This is clearly visualized in the vast number of structures resulting from energetic minima of the ab initio calculations postulated by Reimers and Hall[1] in CH_3CN-H_2O mixtures. In Figure 6C, the correlation coefficient (R^2) of the viscosity correlation of τ_c is decreased in the intermediate composition region in which a large number of CH_3CN-H_2O structures are possible. The R^2 values are extremely close to 1 when the solution is predominantly CH_3CN, that is, when CH_3CN interactions are predominantly self-interactions. However, as H_2O is added, the R^2 decreases to a

minimum as the number of possible CH_3CN-H_2O structures increases and the microheterogeneity in the system reaches a maximum. As the CH_3CN concentration further decreases, the R^2 again increases closer to 1. In this region, the ratio of CH_3CN to H_2O molecules is small, and one predominant type of CH_3CN-H_2O interaction is likely to prevail, leading to less polydispersity in the species present and a higher R^2 in this composition range.

The changing intercept and slope of the different isocomposition lines in Figure 2 clearly show a deviation from a traditional hydrodynamic model for this system. Following the microscopic hydrodynamic approach presented in eq 3, changes in slope of the viscosity correlations can be related to a change in the McClung−Kivelson constant, κ. McClung and Kivelson have related κ to the ratio of the anisotropic portion of the intermolecular potential to the overall intermolecular forces.[60] Figure 6B shows a steady increase in the slope of the viscosity correlations up to $\chi_{CH_3CN} = 0.84$ followed by a decrease until the composition reaches pure CH_3CN, corresponding to a respective increase and decrease of κ in these composition ranges. If we interpret these changes in slope in terms of κ, then it follows that the maximum in slope corresponds to the solution composition where the intermolecular potential of CH_3CN is most anisotropic relative to the overall intermolecular forces, or where the average solvation environment around the CH_3CN produces the most torque. This seems reasonable in light of the R^2 results in Figure 6C and our explanation that the minimum at $\chi_{CH_3CN}\sim0.8$ represents a maximum in the polydispersity of structural species. There is little change in slope between the two lowest compositions of $\chi_{CH_3CN} = 0.0369$ and 0.10, and it is interesting to note that Reimers and Hall do not see a Raman signal for "free" CH_3CN below this composition. This is the same composition that researchers have previously proposed as the onset of microheterogeneity because of the unlikely occurrence of CH_3CN-CH_3CN interactions below this composition. As mentioned previously, one can also interpret the changing slopes of the viscosity correlations using a hydrodynamic volume argument in which the volume of the rotating species (V_h) is not equal to its actual molecular volume (V_m), but is modified due to the fact that strict stick boundary conditions do not apply to the system. In these terms, our slope data indicates an increase in the hydrodynamic volume of the CH_3CN solute as CH_3CN is added to the system up to $\chi_{CH_3CN} = 0.84$ due to the changing boundary conditions of the system, and a subsequent decrease as the solution approaches pure CH_3CN. It is also important to mention that these changing slopes could be attributed to the fact that the quadrupole coupling constant (χ) is not constant as a function of the solution composition. As mentioned, Farrar and co-workers[106−116] have investigated methods for determining changes in χ as a function of temperature and solvent composition in a number of systems. Though they have not examined these changes as a function of solution composition specifically in CH_3CN-H_2O mixtures, in light of the variety of systems investigated, we feel it is important to mention the possibility that this parameter is not a constant.

Examining the intercept data in Figure 6B, it is easily seen that it correlates closely to the R^2 and slope data shown in Figure 6C and 6A, decreasing to $\chi_{CH_3CN}\sim0.8$, where it actually becomes negative, and then increasing up to pure CH_3CN. The existence of an intercept has been interpreted as the correlation time for the free rotor as mentioned previously; however, Kivelson and Madden have noted that the presence of a positive intercept may exist due to the examination of a limited η/T range, and that a linear trend may be part of a larger nonlinear trend existing at lower η/T.[127] They also mention that negative intercepts have been reported for nonrigid molecules, but considering the small size of CH_3CN, this explanation for the data in Figure 6B does not seem plausible. Nevertheless, it is clear that the intercept changes similarly to the other experimental observables, and we feel that it is conceivable that this is also due to changes in the solute−solvent interactions in these mixtures and the microheterogeneity of the solution. Though one would not expect that these changes in experimental observables would be correlated to the solution behavior, we find it intriguing that the changes in all three are related and that these changes seem to be explainable in terms of continuous microheterogeneity.

Within the framework of the two-state model for CH_3CN-H_2O mixtures, it is possible to write an equilibrium constant (K) that represents the reaction in which one CH_3CN-CH_3CN interaction and one H_2O-H_2O interaction are broken to form two CH_3CN-H_2O species. This equilibrium constant can be written in the form

$$K = \frac{(\chi_{CH_3CN_{bound}})^2}{(\chi_{CH_3CN_{free}})(\chi_{H_2Ofree})} \qquad (6)$$

where $\chi_{CH_3CNbound}$ and $\chi_{CH_3CNfree}$ represent the mole fractions of bound and free CH_3CN as described previously, and χ_{H_2Ofree} represents the amount of H_2O *not* bound to CH_3CN. Using the temperature-dependent data in Figure S1 (with maximum bound CH_3CN occurring at $\chi_{CH_3CN} = 0.157$ and maximum free CH_3CN at $\chi_{CH_3CN} = 1.0$), we have calculated K at each mole fraction investigated. Resulting van't Hoff plots ($\ln K$ vs T^{-1}) were made for all of the present thermodynamic conditions examined. The plots obtained were linear only in the intermediate composition region ranging from CH_3CN mole fraction 0.296−0.627, and we should note that there was no distinct trend in these thermodynamic parameters as a function of composition. Although this model does not allow an overall view of the solution structure, it does allow us to estimate the enthalpy (ΔH) and entropy (ΔS) of formation of a CH_3CN-H_2O hydrogen bonded complex. In Figure 7, we plot $\ln K$ versus $1000/T$ for $\chi_{CH_3CN} = 0.390$.

Using the familiar van't Hoff analysis we have determined from the slope and intercept that $\Delta H = 5.80$ kcal/mol and $\Delta S = -19.9$ kcal/mol. In the mole fractions where linear fits were possible, ΔH values ranged from 5.80 to 7.26 kcal/mol and ΔS values ranged from −19.9 to − 25.4 kcal/mol-K, with correlation coefficients ranging from 0.90 to 0.99. The ΔH values are calculated adopting a similar model to that used by Reimers in which two CH_3CN-H_2O interactions are formed from the breaking of one CH_3CN-CH_3CN and one H_2O-H_2O interaction and other interactions involving the molecules remaining intact. Reimers presents the binding energies for several structures from ab initio calculations that include either one CH_3CN-H_2O interaction or two CH_3CN molecules interacting with one H_2O molecule. The binding energies for the single

(127) Kivelson, D.; Madden, P. A. *Annu. Rev. Phys. Chem.* **1980**, *31*, 523−558.

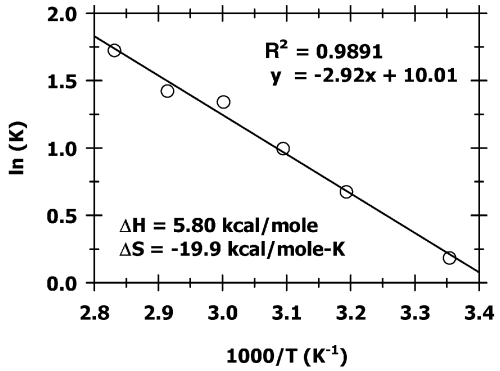

Figure 7. The van't Hoff plot for $\chi_{CH_3CN} = 0.390$ determined using the equilibrium model shown in Equation 6 and the temperature-dependent data in Figure S1.

interaction species range from −1.48 to −3.53 kcal/mol, and from −5.48 to −10.36 kcal/mol for the species including two CH_3CN and one H_2O molecule. We have made the argument that the polydispersity in the correlation coefficients (R^2) (Figure 6C) from the η/T data shows a number of different solution species to be present in this intermediate composition range. That such a simple model represents the solution equilibria at any composition is remarkable, and considering the similarity between the binding energies and the calculated ΔH values as well as the agreement between the Raman and NMR results, the two studies seem to give a consistent view of the continuous nature of microheterogeneity in this RPLC solvent system.

Conclusions

A complete study of the ^{14}N T_1 relaxation times of CH_3CN in CH_3CN-H_2O solvent mixtures covering a wide range of temperatures over the entire binary composition of the mixture has been conducted. Despite the broad use of ^2H in these types of measurements in the past, ^{14}N has been shown to be a reliable nucleus for these studies, with errors well below those associated with previous ^2H investigations. We have observed a striking correlation between the ^{14}N T_1 of CH_3CN and the viscosity of bulk CH_3CN-H_2O mixtures, showing the applicability of a microscopic hydrodynamic model in describing the bulk solution dynamics of this mixture. This model has also been applied to a typical reversed-phase chromatographic system in which CH_3CN-H_2O is in contact with a C_{18}-bonded stationary phase, and we have shown that CH_3CN exhibits inhibited reorientational dynamics at the surface of this stationary phase, and that there is a greater temperature dependence for the viscosity changes of the surface-associated CH_3CN. The use of a two-state fast exchange model makes the determination of the viscosity of these components near the interface possible, and with improvements in the determination of parameters in this model (such as the "thickness" of the surface-associated solvent layer), we will use this same approach to quantitatively determine viscosity changes in other important analytical systems. We have also used this bulk ^{14}N T_1 relaxation data to provide useful insight into the structure of this mixture. From comparisons between the results in the current study and the existing results of Reimers and Hall, we offer further support for a continuous microheterogeneity model for the structure of CH_3CH-H_2O mixtures. Data showing changes in the activation energy of this process as well as, interestingly, the experimental parameters from our hydrodynamic viscosity correlation plots as a function of composition provide further evidence for a structural model of this mixture in which the microheterogeneous structure varies continuously over the full binary composition range.

Acknowledgment. This material is based on work supported in part by a Department of Education GAANN Fellowship (E.D.D.), the STC Program of the National Science Foundation under Agreement No. CHE-9876674, Merck & Co., Inc., The University of North Carolina startup funds, and Varian NMR.

Supporting Information Available: Explanation of angular dependence of τ_c, figure and discussion of application of Equation 5 to temperature-dependent NMR data, T_1 relaxation data for all compositions and temperatures investigated, van't Hoff data for various compositions (PDF). This material is available free of charge via the Internet at http://pubs.acs.org.

JA027226H